Ab initio study of proper topological ferroelectricity in layered perovskite $La_2Ti_2O_7$

Jorge López-Pérez and Jorge Íñiguez

Institut de Ciència de Materials de Barcelona (ICMAB-CSIC), Campus UAB, 08193 Bellaterra, Spain

(Received 23 December 2010; revised manuscript received 29 March 2011; published 8 August 2011)

We present a first-principles investigation of ferroelectricity in layered perovskite oxide $La_2Ti_2O_7$ (LTO). Our calculations indicate that LTO's high-temperature (1770 K) ferroelectric transition results from the condensation of two soft modes that have the same symmetry and are strongly coupled anharmonically. The leading instability mode essentially consists of rotations of the oxygen octahedra that are the basic building blocks of the perovskite structure; remarkably, because of its particular lattice topology or connectivity, such O_6 rotations give rise to a spontaneous polarization in LTO. The effects discussed thus constitute an example of how nanostructuring – provided here by the natural layering of LTO – makes it possible to obtain a significant polar character in structural distortions that are typically nonpolar. We discuss the implications of our findings as regards the design of multifunctional materials, noting that the observed proper ferroelectricity driven by O_6 rotations provides the ideal conditions to obtain strong magnetoelectric effects.

DOI: 10.1103/PhysRevB.84.075121 PACS number(s): 77.84.−s, 61.50.Ah, 75.85.+t, 71.15.Mb

I. INTRODUCTION

Because of their physical appeal and technological importance, ferroelectrics and related materials have been the object of continued attention for decades.[1–3] Bulk oxides with the ideal perovskite structure – ranging from classic ferroelectric $BaTiO_3$ (BTO) to strong dielectric $Ba_{1-x}Sr_xTiO_3$, or from piezoelectric $PbZr_{1-x}Ti_xO_3$ (PZT) to relaxor $(PbMg_{1/3}Nb_{2/3}O_3)_{1-x}$-$(PbTiO_3)_x$ – have been especially well studied. Indeed, partly thanks to a number of key contributions from first-principles theory,[4] we now understand the fundamental atomistic origin of the ferroelectric (FE) and response properties of the most important members of this family. During the past decade, the focus has increasingly shifted toward nanostructured materials, especially in the form of thin films. Work on films has led to a better understanding of how elastic (i.e., the epitaxial strain exerted by a substrate) and electric (e.g., the imperfect screening of the depolarizing field associated with particular metallic electrodes) boundary conditions affect the FE state.[5] Further, it has been shown that exotic FE properties can be obtained in artificially created superlattices, e.g., in the recently discussed $PbTiO_3$/$SrTiO_3$ heterostructures.[6]

The emergence of magnetoelectric (ME) multiferroics[7] (i.e., materials with coupled magnetic and FE orders) has contributed to refuel interest in ferroelectrics, especially in what regards *unconventional* mechanisms for ferroelectricity. If we restrict ourselves to oxides with the ideal ABO_3 perovskite structure, ferroelectricity (usually driven by a *B*-site transition metal with an nd^0 electronic configuration) and magnetism (which requires localized *d* or *f* electrons) seem to be mutually exclusive, the known exceptions being very scarce.[8,9] So far, the most notable ways around this problem consist of i) having ferroelectricity driven by the *A*-site cation, as in room-temperature multiferroic $BiFeO_3$,[10] and ii) moving away from the ideal perovskite structure and resorting to other mechanisms for ferroelectricity, e.g., in the improper FE $YMnO_3$[11,12] and the so-called *hybrid* improper FE $Ca_3Mn_2O_7$.[13]

This is the context of our work on the layered perovskite oxide $La_2Ti_2O_7$ (LTO), whose structure is sketched in Fig. 1. LTO is one of the highest-temperature ferroelectrics known, with a Curie point (T_C) of approximately 1770 K,[14] and is lately being considered for applications as a high-*T* piezoelectric.[15,16] There are other simple (e.g., $LiNbO_3$ with $T_C \approx 1480$ K) and layered (e.g., $Sr_2Nb_2O_7$ with $T_C \approx 1610$ K) perovskites with high Curie temperatures comparable to LTO's. Yet, it is worth noting that LTO's T_C seems enormous when compared with the FE transition temperature of cubic perovskite titanates that share with it the same building blocks, i.e., TiO_6 octahedral groups: Most significantly, BTO becomes FE at about 400 K, and the related compound $SrTiO_3$ remains (a quantum) paraelectric (PE) down to 0 K. Thus, the questions we would like to answer are these: What is the mechanism for ferroelectricity in LTO? How does it differ from what occurs in materials as well known as BTO, so that its Curie temperature is comparatively so high? In principle, two scenarios are possible. LTO might owe its high T_C to the kind of mechanisms known to operate in the cubic titanates (in essence, long-range dipole-dipole interactions that destabilize the nonpolar phase[17,18]), which might somehow be enhanced by the peculiar topology or connectivity of the LTO lattice. Alternatively, LTO might present some different form of very strong FE instability. Either way, the study of this compound will provide us with information that will be useful to better understand ferroelectricity in layered perovskites and eventually design new ferroelectric materials.

Let us also note that LTO is a member of the family of oxides with the general formula $La_nTi_nO_{3n+2}$,[19] whose structure can be seen as the ideal cubic perovskite periodically truncated along the $[011]_c$ direction of the cubic lattice, *n* being the number of perovskite-like planes within one layer (see Fig. 1). These structures are thus related to the well-known Ruddlesden–Popper, Aurivillius, and Dion–Jacobson families of layered perovskites,[20] for which the truncation direction is $[001]_c$ and which include very famous members such as $(La,Ba)_2CuO_4$, the parent compound of high-T_C superconductors. The basic features of the electronic structure of the $La_nTi_nO_{3n+2}$ compounds are controlled by *n*: The La and O atoms can be assumed to be in their most common

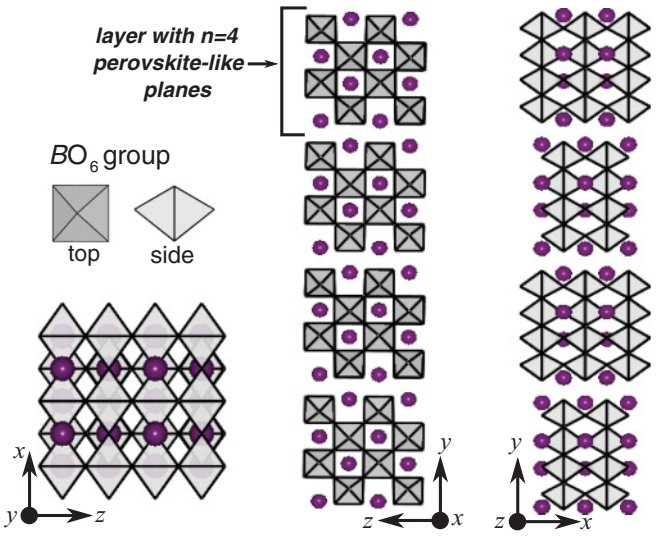

FIG. 1. (Color online) Different views of the layered perovskite structure of the $A_nB_nO_{3n+2}$ compounds for $n = 4$, where n is the number of perovskite-like planes within a layer. Only the A atoms (as balls) and BO_6 octahedra are shown. The defined Cartesian axes x, y, and z (which follow the convention adopted in Ref. 34) are used throughout the paper.

ionization states – i.e., La^{3+} and O^{2-} – which implies that the Ti cations will present a positive charge of $3 + 4/n$. Accordingly, the number of $3d$ electrons in the Ti atoms will be $1 - 4/n$, which allows us to move quasi-continuously from the Ti-$3d^0$ configuration of the $n = 4$ compound (that is our LTO, the family member with smallest n reported in the literature) to the Ti-$3d^1$ configuration of the $n = \infty$ compound (which has the prototype perovskite structure). The variety of electronic phenomena observed for intermediate values of n – including phases of semiconducting, normal metallic, and low-dimensional metallic character[19] – constitutes an additional motivation to study in detail the structural behavior of the relatively simple end member LTO.

The paper is organized as follows. In Sec. II we describe the theoretical approach and first-principles methods used in this work. We present and discuss our results in Sec. III, which is split in the following way. In Sec. III A we describe our results for the structure of the high-temperature PE and FE phases of LTO. In Sec. III B we show that the PE phase presents a strong FE instability whose *topological* nature is discussed in detail. Our results thus show that ferroelectricity in LTO has the same origin as in the barium fluorides $BaMF_4$ (where M is a transition metal), which belong to the same structural family but with $n = 2$.[21] In Sec. III C we describe the phase transition between the PE and FE phases and discuss the energetics of the transformation. In Sec. III D we present our results for the spontaneous polarization, dielectric, and piezoelectric properties. Having described LTO's basic FE properties, which are contrasted with the behavior of prototype compound BTO, in Sec. III E we show that LTO also presents some features that are clearly reminiscent of the usual FE oxides with the ideal perovskite structure. In Sec. III F we outline the implications that our results have for the design of novel ME materials. Finally, in Sec. IV we summarize and present our conclusions. Whenever possible, we compare our first-principles results with the (scarce) experimental information available for LTO.

II. METHODOLOGY

A. Theoretical approach to $La_2Ti_2O_7$

We adopted the usual first-principles approach to the investigation of structural phase transitions of the displacive type, which is routinely applied with great success to FE perovskite oxides.[22] In essence, one needs to identify a reference equilibrium phase of high symmetry (HS) – which corresponds to the high-temperature PE phase of the compound – and study its stability against all possible structural distortions. More precisely, we write the energy of the crystal as the following Taylor series:

$$E = E^0 + \frac{1}{2}\sum_{m,n} K_{mn}u_m u_n + \mathcal{O}(u^3), \qquad (1)$$

where E^0 is the energy of the HS phase. The u_m variables represent the structural distortions of the reference configuration; for the study of a FE transition, one can typically restrict oneself to the distortions compatible with the reference unit cell, i.e., those associated with the Γ point of the Brillouin zone of the PE phase. The so-called *force-constant matrix* $\boldsymbol{K}$ is the central quantity one needs to compute, as its negative eigenvalues (if any) correspond to unstable structural distortions – i.e., *soft* modes – that may result in a phase transition. Let us use the term *mode stiffness* to refer to the eigenvalues of $\boldsymbol{K}$, which we denote by κ_s, with s running from 1 to the dimension of the force-constant matrix. Note that the magnitude of a negative κ_s determines the *strength* of the structural instability, and thus the likelihood of observing it experimentally. (In general, one may find several, possibly competing, instabilities of a HS phase; it is by no means guaranteed that all of them will lead to experimentally observable phase transitions.) Once a soft-mode is identified, one can readily study the corresponding low-symmetry (LS) phase – by distorting the crystal according to the soft-mode eigenvector and relaxing the resulting structure – and the energetics of the instability – by computing the usual double-well potential connecting the HS and LS phases.

To apply this program to LTO, we had to tackle one fundamental difficulty: We could not find any experimental information on the structure of the high-temperature PE phase of this compound.[23] Note that this is never a problem when one works with the usual FE perovskites, where the ideal cubic perovskite structure is the reference phase of choice. Such a choice is obviously correct in cases like those of BTO or $PbTiO_3$, where the cubic PE phase is experimentally accessible for $T > T_C$; more remarkably, this choice is also the most physically sound one for materials (e.g., $BiFeO_3$) whose cubic PE phase is not easy to access experimentally, as the samples tend to melt before reaching the corresponding transition temperature. In the general case, the problem of choosing an appropriate HS reference phase for the theoretical study of displacive phase transitions has long been solved. The basic idea is to look for *pseudo-symmetries* (i.e., *slightly* broken symmetries) of the known LS structure; we can thus identify possible HS phases that would transform into the

known LS structure upon a relatively small distortion. This is a very powerful strategy that can lead to the discovery of complex phase-transition sequences (e.g., when more than one possible HS phase is found) and, in particular, has been used to identify previously unnoticed FE transitions.[24,25]

Using widely available crystallographic tools,[26] we applied the pseudo-symmetry analysis to LTO and obtained a very clear prediction: We found that the FE phase of this compound, which presents space group $Cmc2_1$ and a 22-atom primitive unit cell, is most likely associated with a PE phase with the same primitive cell and space group $Cmcm$ (see sketch in Fig. 2). We thus performed our first-principles study using this $Cmcm$ phase as our HS reference structure.

A few additional points are in order: (1) The pseudo-symmetry analysis resulted in relatively large atomic displacements connecting the HS and LS phases, with maximum values of about 0.4 Å corresponding to the La atoms. Note that the magnitude of such distortions is expected to reflect the associated HS-LS transition temperature,[27] which is indeed very high in this case. (2) Experimental studies of the compounds $Sr_2Nb_2O_7$ and $Ca_2Nb_2O_7$,[28,29] which share with LTO the same layered structure and a similar (nd^0) electronic configuration of the transition-metal atoms, show that they present a high-temperature phase with the $Cmcm$ space group. (3) The choice of $Cmcm$ as our PE space group results in specific predictions for the symmetry of the soft modes that would be associated with a FE transition to the $Cmc2_1$ phase. Indeed, the leading instability should transform with the B_{1u} irreducible representation of mmm, the point group of the $Cmcm$ phase. As we will see, our first-principles results confirmed these expectations, thus supporting our choice of space group for the PE phase.

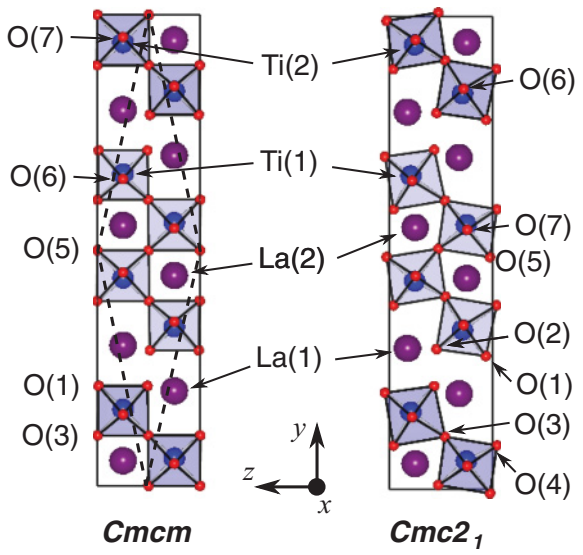

FIG. 2. (Color online) Structures of the $Cmc2_1$ (FE) and $Cmcm$ (PE) phases of $La_2Ti_2O_7$ studied in this paper. The small (red), medium (blue), and big (violet) balls represent O, Ti, and La atoms, respectively. The shaded polyhedra are top-viewed O_6 groups. The two phases have the same 44-atom conventional cell depicted in the figure; the 22-atom primitive cell, which is also common to both, is indicted with dashed lines in the $Cmcm$ case. The defined Cartesian axes x, y, and z (which follow the convention adopted in Ref. 34) are used throughout the paper. The symmetry-independent atoms are labeled as in Table I; note that oxygens O(1) and O(3) of the $Cmcm$ structure split, respectively, into O(1)/O(2) and O(3)/O(4) in the $Cmc2_1$ structure.

Finally, in this paper we make a brief reference to a lower-temperature phase of LTO that presents the $P2_1$ space group.[14,30] Let us note that the $Cmc2_1$-to-$P2_1$ transition involves the doubling of the orthorhombic cell along the x direction, and thus involves a structural distortion associated with a $\boldsymbol{q}$ point different from Γ. Such instabilities were not considered in the present paper.

B. Details of the calculations

We used the local density approximation (LDA) to density functional theory (DFT) as implemented in the first-principles Vienna *ab initio* simulation package (VASP).[31] To represent the ionic cores we used the projector-augmented wave scheme,[32] solving explicitly for the following electrons: La's $5p$, $5d$, and $6s$; Ti's $3p$, $3d$, and $4s$; and O's $2s$ and $2p$. The electronic wave functions were represented in a plane-wave basis truncated at 400 eV. We always worked with the 44-atom cell of LTO sketched in Fig. 2 (which is the conventional cell for both $Cmcm$ and $Cmc2_1$ phases), and used a $6 \times 1 \times 5$ k-point grid for Brillouin zone integrations. We checked that these calculation conditions were well - converged by monitoring the computed equilibrium structure, bulk modulus, and phonon frequencies of the $Cmcm$ phase. For the calculation of the force-constant matrix $\boldsymbol{K}$ and the dielectric and piezoelectric responses, we employed a simple finite-displacement scheme and the corresponding linear-response tensor formulas, which can be found, e.g., in Ref. 33. We only computed the lattice-mediated part of the static dielectric response, which has been repeatedly shown to dominate the effect in FE oxides.

Our BTO simulations were analogous to the above described ones. We solved explicitly for Ba's $5s$, $5p$, and $6s$ electrons (treating Ti and O as above), and used a 400 eV cutoff for the plane-wave basis. We worked with the 5-atom unit cell of BTO and used a $6 \times 6 \times 6$ k-point grid for Brillouin zone integrations.

III. RESULTS AND DISCUSSION

A. Structure of the $Cmcm$ and $Cmc2_1$ phases

Table I shows our results for the equilibrium structure of the $Cmcm$ (PE) and $Cmc2_1$ (FE) phases of LTO considered in this paper. For $Cmc2_1$ we also report the experimental structure measured at 1173 K by Ishizawa *et al.*[34] using x-ray diffraction.

While the overall agreement between the experimental and theoretical FE structures is acceptable, the deviations affecting some atomic positions and lattice constants are larger than what is usual for this type of calculations. For example, the predicted position of the La(1) atom differs notably from the experimentally determined one; more significantly, the computed a and c lattice constants deviate from the experimental values by almost 3%. We attribute these discrepancies to the fact that we are comparing our first-principles results, which correspond to the limit of 0 K, with structural data taken at very high temperatures. Given that thermal expansion and other temperature-driven effects are not included in our

TABLE I. Computed equilibrium structures of the *Cmcm* and $Cmc2_1$ phases of LTO discussed in the text. We show in parentheses the experimental values reported in Ref. 34 for the $Cmc2_1$ phase.

Cmcm	$a = 3.891$ Å	$b = 25.720$ Å	$c = 5.465$ Å	
	$\alpha = \beta = \gamma = 90^\circ$			
Atom	Wyc.	x	y	z
La(1)	4*c*	0	0.2924	1/4
La(2)	4*c*	0	0.4453	3/4
Ti(1)	4*c*	1/2	0.3389	3/4
Ti(2)	4*c*	1/2	0.4437	1/4
O(1)	8*f*	1/2	0.2881	0.9931
O(3)	8*f*	1/2	0.3982	0.9869
O(5)	4*a*	1/2	1/2	1/2
O(6)	4*c*	0	0.3458	3/4
O(7)	4*c*	0	0.4525	1/4
$Cmc2_1$	$a = 3.845$ Å	$b = 25.626$ Å	$c = 5.464$ Å	
	($a = 3.954$ Å	$b = 25.952$ Å	$c = 5.607$ Å)	
	$\alpha = \beta = \gamma = 90^\circ$			
Atom	Wyc.	x	y	z
La(1)	4*a*	0	0.2978	0.1675
			(0.2981)	(0.1757)
La(2)	4*a*	0	0.4464	0.7515
			(0.4461)	(0.7500)
Ti(1)	4*a*	1/2	0.3369	0.7069
			(0.3370)	(0.7095)
Ti(2)	4*a*	1/2	0.4407	0.2422
			(0.4404)	(0.2452)
O(1)	4*a*	1/2	0.2803	0.9245
			(0.2818)	(0.9350)
O(2)	4*a*	1/2	0.2960	0.4399
			(0.2964)	(0.4580)
O(3)	4*a*	1/2	0.3843	0.0415
			(0.3891)	(0.0390)
O(4)	4*a*	1/2	0.4072	0.5549
			(0.4077)	(0.5420)
O(5)	4*a*	1/2	0.4905	0.9724
			(0.4912)	(0.9750)
O(6)	4*a*	0	0.3460	0.7426
			(0.3472)	(0.7200)
O(7)	4*a*	0	0.4507	0.2604
			(0.4511)	(0.2550)

simulations, our results seem compatible with the experimental information.

B. Ferroelectric instabilities of the *Cmcm* phase

As described in Sec. II A, we studied the structural stability of the *Cmcm* phase against Γ-point distortions (compatible with the PE unit cell) by computing the corresponding force-constant matrix $\boldsymbol{K}$. From the diagonalization of $\boldsymbol{K}$ we obtained two negative eigenvalues that correspond to two structural instabilities. The computed mode stiffnesses are -0.81 and -0.01 eV/Å^2, respectively. Hence, according to our calculations, LTO's *Cmcm* phase presents a structural instability comparable in strength to the FE soft mode of BTO's PE phase (for which we obtained -2.74 eV/Å^2), as well as a marginally unstable mode with nearly zero stiffness.

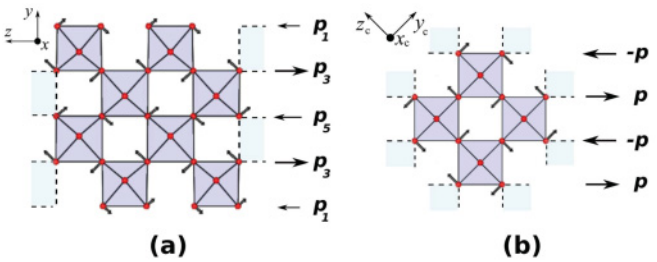

FIG. 3. (Color online) (a) Sketch of the largest atomic displacements associated with the strongest instability mode ($\boldsymbol{\xi}_1$) obtained for the *Cmcm* phase of LTO. We show the displacements corresponding to one layer composed of $n = 4$ perovskite-like planes. The arrows on the side represent the electric dipoles associated to the displacement of oxygens in different y-planes (see text). The dipoles are labeled as the oxygen atoms in Fig. 2. (b) Sketch of a typical anti-ferrodistortive mode occurring in an ideal (non-layered) perovskite structure.

Both instabilities transform with the B_{1u} irreducible representation of the *mmm* point group of the PE phase; more precisely, they are infrared active (polar) modes that involve the development of a polarization along the z direction defined in Fig. 2. Such B_{1u} modes break the C_{2y}, C_{2x}, I, and σ_z point symmetries of the PE phase (where I is the spatial inversion, $C_{2\alpha}$ stands for a twofold rotation around axis α, and σ_α is a mirror plane perpendicular to direction α), leading to the $Cmc2_1$ space group. Hence, the obtained B_{1u} soft modes are exactly the kind of instabilities that can drive a FE phase transition between the *Cmcm* and $Cmc2_1$ phases. Our first-principles results thus support the correctness of our working hypothesis, i.e., that the studied *Cmcm* structure is indeed the HS PE phase of LTO.

We can gain insight into the origin of ferroelectricity in LTO by inspecting the eigenvector of the strongest instability mode, denoted by $\boldsymbol{\xi}_1$ in the following. In essence, $\boldsymbol{\xi}_1$ involves a rotation of the O_6 oxygen octahedra around the x axis, as sketched in Fig. 3(a). Hence, the displacements of the equatorial oxygens amount to most of the eigenvector [11% of the norm of $\boldsymbol{\xi}_1$ is associated with O(1) displacements, 51% with O(3), and 28% with O(5), using the labels defined in Fig. 2 for the oxygen atoms]; there are also significant La displacements (9% of the norm), while the Ti atoms and apical oxygens O(6) and O(7) have a negligible participation in $\boldsymbol{\xi}_1$. The character of the second soft mode ($\boldsymbol{\xi}_2$) is more complex: It is dominated by the displacements of oxygens O(1) and O(5) (with 21% and 35% of the norm, respectively) and involves a significant deformation of the O_6 octahedra; it also presents a large participation of the La atoms (about 24% of the norm).

These FE instabilities are very different from the ones that are usual among ABO_3 oxides with the ideal perovskite structure. The inset of Fig. 4(b) shows the representative case of BTO: The Ti cation moves away from the center of the O_6 octahedron, which is only slightly distorted, giving rise to a large electric dipole. Further, the FE instability in BTO and related materials is known to originate from the strong interactions between such local dipoles.[18] In contrast, the dominant FE instability found in LTO consists of O_6 octahedra rotations, the off-centering of the Ti atoms being negligible. As

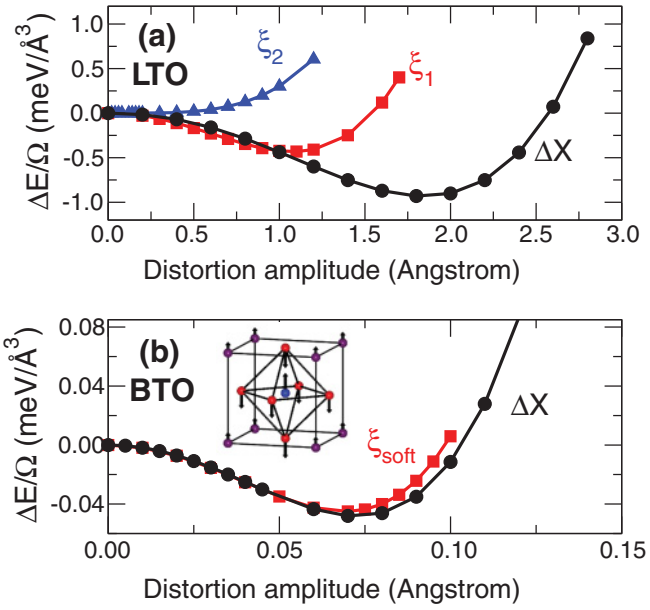

FIG. 4. (Color online) (a) Variation of the energy of LTO as the $Cmcm$ phase is distorted according to several atomic displacement patterns, namely, those corresponding to the soft modes $\boldsymbol{\xi}_1$ and $\boldsymbol{\xi}_2$, as well as the distortion $\Delta \boldsymbol{X}$ that connects the $Cmcm$ and $Cmc2_1$ phases. The 44-atom cell of the $Cmcm$ phase is kept fixed in all calculations. (b) Same as panel (a) for the PE ($Pm\bar{3}m$) to FE ($P4mm$) transition of BTO. The inset shows the atomic displacements associated with the single FE soft mode of BTO (Ba atoms at the corners of the cubic cell; Ti atom at the center of the O_6 octahedron). For both LTO and BTO, the energies are normalized to the volume of the PE phase so that a comparison between compounds can be made.

quantified in Sec. III D, such a pattern of atomic displacements does not lead to a large local dipole, which suggests that the mechanisms responsible for the ferroelectricity in LTO have to be of a different nature.

Interestingly, structural instabilities involving O_6 octahedra rotations are very common among ABO_3 perovskites, and are usually termed antiferrodistortive (AFD). Indeed, AFD modes such as the one sketched in Fig. 3(b) are the driving force for most of the structural phase transitions occurring in these compounds, the examples including crystals as well-known as $SrTiO_3$, $LnMnO_3$ and $LnNiO_3$ (where Ln is a lanthanide), multiferroics $BiMO_3$ (where M is a $3d$ transition metal), etc. Accordingly, there is extensive literature devoted to the study and classification of AFD modes in ABO_3 perovskites,[35–38] and it is known that size (e.g., the incompatibility of the ionic radii of the A and B cations to form a cubic perovskite lattice) and chemical (as in the Bi-based compounds that display the so-called *stereochemical activity*) effects are usually responsible for the occurrence of AFD distortions.[39] Hence, it is not a surprise to find that layered perovskite structures may present AFD-like instabilities that allow for a better fulfillment of steric and/or chemical constraints at a local level. It is not our goal here to discuss the occurrence and origin of such soft modes in LTO-like layered perovskites; such a study should probably involve consideration of a number of representative crystals (e.g., a few members of the $A_nB_nO_{3n+2}$ family) and falls beyond the scope of this paper. Suffice it to say that the leading FE instability that we found in LTO is essentially analogous to the AFD distortions that are ubiquitous among perovskite oxides.

However, we must note a critical difference between LTO's AFD-like mode depicted in Fig. 3(a) and the AFD modes occurring in ideal perovskite structures [Fig. 3(b)]: The former causes a spontaneous polarization, while the latter do not. To better explain this, in Fig. 3(a) we indicate with arrows the electric dipoles that appear as a consequence of the displacement of the oxygen atoms following the $\boldsymbol{\xi}_1$ eigenvector. The oxygens in each y-oriented plane give rise to a dipole along the z direction. Using the definitions in Fig. 3(a), the total dipole associated with one layer would be $\boldsymbol{p}^{\text{layer}} = 2\boldsymbol{p}_1 + 2\boldsymbol{p}_3 + \boldsymbol{p}_5$. Since there is no symmetry relationship between the displacements of the O(1), O(3), and O(5) oxygens in the $\boldsymbol{\xi}_1$ eigenvector, it follows immediately that the $\boldsymbol{p}^{\text{layer}}$ will be different from zero. Moreover, even if oxygens of different types were to displace by the same amount, so that $\boldsymbol{p}_1 = -\boldsymbol{p}_3 = \boldsymbol{p}_5 = \boldsymbol{p}$, we would still have $\boldsymbol{p}^{\text{layer}} = \boldsymbol{p} \neq 0$, as the number of oxygen planes in each layer is odd. Finally, note that LTO's unstable mode $\boldsymbol{\xi}_1$ involves an identical distortion of all layers in the structure, and thus gives rise to a net macroscopic polarization.

On the other hand, AFD distortions of the ideal (nonlayered) perovskite structure do not result in a macroscopic polarization. In Fig. 3(b) we show a pattern of O_6 rotations around the indicated x_c axis; the situation is very similar to the one depicted in Fig. 3(a), except that in this case the network of O_6 octahedra is not truncated. Again, we indicate with arrows the electric dipoles that appear as a consequence of the oxygen displacements: oxygens within a $[011]_c$-oriented plane give rise to a dipole $\boldsymbol{p}$ along $[01\bar{1}]_c$. It is apparent that the addition of all such dipoles gives no net polarization in this case, a result that can be viewed as a consequence of the three-dimensional nature of the O_6 network.

In conclusion, we have found that the strongest structural instability in LTO's HS phase is a very common and simple one: It involves concerted rotations of the O_6 octahedra, much like the AFD modes responsible for the structural phase transitions in most ABO_3 crystals with the ideal perovskite structure. AFD distortions in the usual perovskites are well known to be nonpolar, a feature that can be viewed as a consequence of the symmetry and three-dimensional character of the lattice. In contrast, because the structure of LTO is split in layers comprising an even number of perovskite-like planes, the O_6-rotation mode gives rise to a net polarization in this case. Hence, since the occurrence of a spontaneous polarization in LTO relies on the layered topology of the lattice, it seems appropriate to describe this compound as a *topological ferroelectric*. Let us stress that LTO's peculiar lattice topology does not seem essential for the structural instability to exist, but it is critical for it to have a polar character.

Interestingly, LTO's topological ferroelectricity is in essence identical to what Ederer and Spaldin described as *geometric ferroelectricity* in the multiferroic fluorides $BaMF_4$, where M = Mn, Fe, Co, or Ni.[21] (We find it more appropriate to use the terms "lattice topology" or "lattice connectivity" to refer to the "geometric constraints" of Ref. 21.) Indeed, the $BaMF_4$ compounds belong to the same layered-perovskite family as LTO; more specifically, they have an $n = 2$ layered

structure that, as far as we know, does not occur among oxides. As shown in Ref. 21, the FE transition in these compounds is characterized by a single soft mode with a strong O_6-rotational character; hence, it bears obvious similarities with what we find occurs in LTO.

C. Nature of the *Cmcm*-to-*Cmc*2_1 transition

In addition to the already discussed topological nature of the leading FE instability, the transformation between LTO's *Cmcm* and *Cmc*2_1 phases presents a number of interesting aspects that we discuss in the following. Most importantly, our results indicate that the transition is driven by the combined action of the two soft modes discussed in Sec. III B and suggest that such a cooperation is critical for it to occur at a very high temperature.

To study a structural phase transition quantitatively, one can start by comparing the energies of the phases involved. Table II shows our results for LTO, along with the analogous data for the $Pm\bar{3}m$ (PE) and $P4mm$ (FE) phases of BTO. Note that the energy change *per* unit volume involved in LTO's transition is about one order of magnitude greater than the corresponding one for BTO. Such an enormous difference is compatible with the experimentally measured Curie temperatures, which are 1770 and 400 K for LTO and BTO, respectively. Hence, our first-principles results for the energetics of LTO's FE transition seem consistent with experiments.

Table II also contains information about the elastic deformation that accompanies the FE transitions. The properties of FE oxides with the ideal perovskite structure are known to be strongly sensitive to cell strains. This is clearly reflected in the results for BTO: If the compound is forced to keep the cubic cell of the PE structure, the energy gain involved in the FE transition is reduced by half (i.e., it drops from -0.110 to -0.051 meV/Å^3). On the other hand, if we impose only the PE volume (so that the FE cell is allowed to deform and acquire a $c/a \neq 1$ ratio), the energetics of the transformation is not strongly affected. In contrast, the analogous elastic constraints have a relatively small effect in the case of LTO (i.e., the energy gain drops from -1.097 to -0.938 meV/Å^3 when we impose the PE cell). Such a weak coupling between strain and the FE distortion is probably reflecting the AFD-like character of the instability;[40] this result also suggests that LTO will display relatively small piezoelectric effects as compared with regular FE perovskites.

TABLE II. Energy difference between the FE and PE phases of $La_2Ti_2O_7$ and $BaTiO_3$. The FE phases are considered under several elastic constraints (see text), which we denote as fully relaxed (no constraint), PE volume, and PE cell. For both LTO and BTO, the energies are normalized to the volume of the PE phase so that a comparison between compounds can be made. Results given in meV/Å^3.

Phase	LTO	BTO
Fully-relaxed	-1.097	-0.110
PE volume	-1.042	-0.099
PE cell	-0.938	-0.051

Let us now consider the atomic displacements that characterize the *Cmcm*-to-*Cmc*2_1 transformation. In most materials undergoing displacive transitions, the atomic distortion connecting the HS and LS phases is essentially captured by the eigenvector of the instability mode that triggers the transformation. One can easily quantify this by constructing a *distortion vector* $\Delta\boldsymbol{X}$ comprising all the atomic displacements associated with the HS-to-LS transition, and expressing it in the basis formed by the eigenvectors $\boldsymbol{\xi}_s$ of the force-constant matrix of the HS phase. (For simplicity, we constructed our distortion vectors $\Delta\boldsymbol{X}$ using the atomic positions of a LS phase that is forced to have the same unit cell as the HS phase.) For BTO, this analysis led us to the expected result: The soft mode of the PE phase captures 98% of the atomic distortion involved in the $Pm\bar{3}m$-to-$P4mm$ transition. However, the result for LTO was qualitatively different: The strongest instability mode ($\boldsymbol{\xi}_1$, with $\kappa_1 = -0.81$ eV/Å^2) captures 81% of the total distortion, and the second instability mode ($\boldsymbol{\xi}_2$, with $\kappa_2 = -0.01$ eV/Å^2) contributes with 15%. (For both compounds, no other mode contributes more than 1%.) Hence, our results suggest that the two soft modes $\boldsymbol{\xi}_1$ and $\boldsymbol{\xi}_2$ play an important role in LTO's FE phase transition.

Such a large contribution of $\boldsymbol{\xi}_2$ to the structural transformation seems incompatible with the computed mode stiffnesses; indeed, the values of κ_1 and κ_2 would suggest that $\boldsymbol{\xi}_2$ is about 80 times weaker than $\boldsymbol{\xi}_1$ as an instability. To resolve this apparent contradiction, we computed how LTO's energy changes when the *Cmcm* phase is distorted according to the individual $\boldsymbol{\xi}_1$ and $\boldsymbol{\xi}_2$ modes. As shown in Fig. 4(a), we found a large energy reduction associated with the $\boldsymbol{\xi}_1$ distortion, while the $\boldsymbol{\xi}_2$ instability is almost negligible. We also computed the energy variation as the total distortion $\Delta\boldsymbol{X}$ is frozen in. Remarkably, as compared with the results for $\boldsymbol{\xi}_1$, the $\Delta\boldsymbol{X}$ curve in Fig. 4(a) presents a much deeper minimum corresponding to a much larger distortion amplitude. This is a new indication that the $\boldsymbol{\xi}_1$ soft mode cannot explain LTO's FE transition by itself. This result contrasts with the situation for BTO [Fig. 4(b)], where the FE soft mode captures the energetics of the structural transformation almost exactly.

The results of Fig. 4(a) suggest that there is a strong and *cooperative* coupling between the two instability modes of LTO. To better describe this effect, let us write the energy of the crystal as the following Taylor series:

$$E = E^{Cmcm} + \tfrac{1}{2}\kappa_1 u_1^2 + \tfrac{1}{2}\kappa_2 u_2^2 + \tfrac{1}{4}\alpha_1 u_1^4 + \tfrac{1}{4}\alpha_2 u_2^4 + \gamma' u_1^3 u_2 + \gamma'' u_1^2 u_2^2 + \gamma''' u_1 u_2^3 + \mathcal{O}(u^6), \qquad (2)$$

where E^{Cmcm} is the energy of the *Cmcm* phase, and u_1 and u_2 are, respectively, the amplitudes (in angstroms) of the $\boldsymbol{\xi}_1$ and $\boldsymbol{\xi}_2$ distortions. Note that this expression for the energy is greatly simplified by symmetry and that the quadratic parameters coincide with the mode stiffnesses. We have included in Eq. (2) only the lowest-order couplings between u_1 and u_2, which are quantified by the primed γ parameters. By fitting to the $\boldsymbol{\xi}_1$ and $\boldsymbol{\xi}_2$ energy curves of Fig. 4(a), we got $\kappa_1 = -0.79$ eV/Å^2 and $\kappa_2 = 0.00$ eV/Å^2, in fair agreement with the values obtained from the diagonalization of $\boldsymbol{K}$; we also got $\alpha_1 = 0.65$ eV/Å^4 and $\alpha_2 = 0.66$ eV/Å^4. Then, to fit the $\Delta\boldsymbol{X}$ curve, we considered distortions characterized by $u_1/u_2 = 0.81/0.15$, as it corresponds to the *Cmc*2_1 phase.

Note that, in this case, the fitted quartic coefficient is a combination of the α and γ parameters of Eq. (2). Given the large u_1/u_2 ratio associated with the $\Delta \boldsymbol{X}$ distortion, and in view of further tests discussed in Sec. III D, it seems reasonable to assume that γ' dominates over γ'' and γ'''; we thus got $\gamma' = -0.35\ \mathrm{eV/\AA^4}$. As compared with the computed α coefficients, this clearly is a very strong anharmonic coupling that favors the combined $\boldsymbol{\xi}_1 + \boldsymbol{\xi}_2$ distortion.[41]

To the best of our knowledge, such a cooperation between soft modes is rare among perovskite oxides.[42] There are many examples of materials in which several strong instabilities exist; in most cases, the strongest one leads to a phase transition that tends to suppress, partially or totally, the other instabilities. The competition between the FE and AFD soft modes in compounds like $SrTiO_3$ is a representative and well-studied case.[43] In contrast, we find that the reciprocal enhancement of the two soft FE modes is critical to explain the structural transformation in LTO. The $\boldsymbol{\xi}_1$ mode is clearly the leading instability, and it would occur even in absence of $\boldsymbol{\xi}_2$. Yet, as the results in Fig. 4(a) show, the magnitude and strength of the transformation are boosted by the interaction between $\boldsymbol{\xi}_1$ and $\boldsymbol{\xi}_2$. Thus, our results seem to suggest that LTO owes its very high T_C to such an interaction; indeed, in view of Fig. 4(a) – which shows that the minimum of the $\Delta \boldsymbol{X}$ curve is more than twice deeper than the minimum of the $\boldsymbol{\xi}_1$ curve – it is hard to imagine LTO's T_C would remain essentially the same if the coupling between $\boldsymbol{\xi}_1$ and $\boldsymbol{\xi}_2$ was suppressed.[44]

Studying from first principles the onset and temperature dependence of the FE distortion(s) of LTO is a challenging endeavor that remains for future work. Nevertheless, a few observations can be made based on the present results. In principle, one could try to approach the problem by introducing a Landau potential of the form

$$F - F_0 = \tfrac{1}{2}A_1(T - T_C)Q_1^2 + \tfrac{1}{4}B_1 Q_1^4 + \tfrac{1}{2}A_2 Q_2^2 + \tfrac{1}{4}B_2 Q_2^4 + C' Q_1^3 Q_2 + C'' Q_1^2 Q_2^2 + C''' Q_1 Q_2^3 , \quad (3)$$

which is written in terms of two one-dimensional order parameters, a primary Q_1 and a secondary Q_2, that have the same symmetry and are strongly coupled anharmonically.[45] In the following heuristic argument, we will consider only the $Q_1^3 Q_2$ crossed term – in accordance with our above conjecture regarding the couplings in Eq. (2) and because this is the most relevant crossed term in the vicinity of the phase transition,[46] – thus assuming that $C'' = C''' = 0$.

If we were dealing with a simple transition, we would have a primary order parameter Q_1 corresponding to the unstable eigenmode of the $\boldsymbol{K}$ matrix of the HS phase; the temperature dependence of the Landau potential would be restricted to the Q_1^2 term, as indicated in Eq. (3), and we would have positive A_1 and B_1 coefficients. Further, a secondary order parameter Q_2 would be stable by itself, with positive A_2 and B_2 coefficients. Hence, the corresponding Landau theory would predict a phase transition at $T = T_C$, with

$$Q_1 = \left[\frac{A_1}{B_1}(T_C - T)\right]^{1/2} \quad (4)$$

below the transition temperature. (The indicated formulas were derived assuming that we remain close to the transition temperature.) Then, Q_2 would present the following temperature dependence below T_C:

$$Q_2 = -\frac{C'}{A_2}Q_1^3 = -\frac{C'}{A_2}\left[\frac{A_1}{B_1}(T_C - T)\right]^{3/2} . \quad (5)$$

In a simple case, the coefficients in Eq. (2) may be a good approximation to the coefficients in Eq. (3) in the limit of low temperatures. Thus, by supplementing Eq. (2) deduced from first principles with a piece of experimental information – i.e., the value of the transition temperature T_C – we could construct the corresponding Landau potential and obtain a quantitative description of the temperature dependence of Q_1 and Q_2.

The doubts quickly appear when one tries to apply this model to LTO. It would seem natural to associate Q_1 and Q_2 with our computed FE soft modes $\boldsymbol{\xi}_1$ and $\boldsymbol{\xi}_2$, respectively. However, that identification implies that the transition temperature for Q_1 is independent of Q_2; such an approximation would be an awkward one, given the large influence that $\boldsymbol{\xi}_2$ has in the energetics of the $Cmcm$-to-$Cmc2_1$ transformation. Additionally, we would be forced to speculate regarding the T dependence of the A_2 coefficient, as our *guess* for this parameter – i.e., the κ_2 of Eq. (2) which was found to be essentially zero – does not comply with the usual requirements for the quadratic coefficient of a secondary mode. Note that, for example, if we had a small value of A_2 and thus a dominant B_2 term, the behavior with temperature of both Q_1 and Q_2 would vary: Q_1 would have the same functional T dependence but with a different prefactor, and Q_2 would go as $(T_C - T)^{1/2}$ instead of $(T_C - T)^{3/2}$.

Hence, as already mentioned, the results of the present study do not allow us to resolve the details of LTO's high-temperature FE transition. Further, as the above discussion illustrates, LTO's case is an especially difficult one, and it is not obvious how to relate the two soft modes obtained from first-principles calculations with the two order parameters that, presumably, should appear in the corresponding Landau theory.

To conclude this section, let us note that complex structural phase transitions involving a variety of modes have been reported for other layered perovskite oxides, such as $SrBi_2Ta_2O_9$ (in which a hard secondary mode is critical to stabilize the FE phase)[47] and the already mentioned $Ca_3Mn_2O_7$ (in which O_6-rotational distortions are involved in the occurrence of ferroelectricity).[13] More work will be needed to establish how general such multimode transformations are and to determine whether the behavior of different structural families admits some sort of unified description.

D. Polarization and response properties

Table III shows the computed spontaneous polarization, lattice-mediated dielectric tensor, and piezoelectric tensor for the $Cmc2_1$ phase of LTO. For comparison, we also show results from the literature corresponding to the $P2_1$ phase that is stable at room temperature.

We obtained a value of 0.29 $\mathrm{C/m^2}$ for the spontaneous polarization, which is comparable to the result of 0.38 $\mathrm{C/m^2}$ that we obtained for the tetragonal phase of BTO. The dielectric response is also very significant, as the obtained values are comparable to those typical of FE perovskites (e.g., we got $\epsilon_{zz} = 23$ for the z-polarized tetragonal phase

TABLE III. Nonzero components of the spontaneous polarization (P_z^S, given in C/m^2), lattice-mediated dielectric tensor ($\epsilon_{\alpha\beta}$), and piezoelectric tensor ($d_{\alpha l}$, where l labels strain components in Voig notation, given in pC/N) of the $Cmc2_1$ phase of LTO. For the dielectric tensor, the clamped-cell response is given in parenthesis.[33] For the piezoelectric tensor, the clamped-ion response is given in parenthesis. We also show experimental[14] and theoretical[16] values for the $P2_1$ phase of LTO that is stable at room temperature (T_{room}). Note that the results in Refs. 14 and 16 have been adapted to our choice of Cartesian axes.

	$Cmc2_1$ phase	$P2_1$ phase	
	this work	Exp. (T_{room})[14]	Theory[16]
P_z^S	0.29	0.05	0.08
ϵ_{xx}	62 (61)	52	–
ϵ_{yy}	44 (44)	42	–
ϵ_{zz}	65 (54)	62	–
d_{z1}	12 (0)	3	–
d_{z2}	4 (1)	6	–
d_{z3}	−22 (0)	16	–
d_{x5}	−2 (0)	–	–
d_{y4}	1 (0)	–	–

of BTO). As regards piezoelectricity, the computed responses are considerable but not particularly large; for example, for the low-temperature rhombohedral phase of BTO, the piezoelectric coefficients reach values of 200 pC/N,[33] while for LTO we got maximum values of about 20 pC/N. LTO's relatively small piezoelectric response seems compatible with the minor role that the cell strains play in determining the energetics of the $Cmcm$-to-$Cmc2_1$ phase transition, as mentioned in the discussion of Table II.

The large spontaneous polarization obtained may seem incompatible with the AFD-like character of the structural instability ($\boldsymbol{\xi}_1$) that dominates the $Cmcm$-to-$Cmc2_1$ transition. To clarify this point, we performed alternative calculations using linear-response expressions[33] based on the Born effective-charge tensors $\boldsymbol{Z}_i^*$ that quantify the polarization change associated with the displacement of an individual atom i.

The polarization reported in Table III was obtained in the standard way: We used the Berry-phase theory of King-Smith and Vanderbilt[48] to compute the variation of $\boldsymbol{P}$ as the $Cmc2_1$ structure is deformed into a symmetry-equivalent one with opposite polar distortion; then, $\boldsymbol{P}^S$ is half of the computed polarization change. $\boldsymbol{P}^S$ can also be estimated using the approximate formula

$$P_\alpha^S \approx \Omega^{-1} \sum_{i\beta} Z^*_{i,\alpha\beta} \Delta X_{i\beta} \,, \tag{6}$$

where $\Delta \boldsymbol{X}$ is the vector capturing the distortion that connects the $Cmcm$ and $Cmc2_1$ phases, Ω is the cell volume, i labels the atoms in the unit cell, and α and β label spatial directions. Using different choices for the effective-charge tensors (i.e., those computed for the $Cmcm$ phase, as well as the corresponding results for the $Cmc2_1$ phase subject to different cell constraints) we obtained values of P_z^S in the 0.25–0.32 C/m^2 range, which are perfectly compatible with the result in Table III.

TABLE IV. Computed effective-charge tensors (given in units of elementary charge) for the $Cmcm$ (PE) and $Cmc2_1$ (FE) phases of $La_2Ti_2O_7$. To facilitate the comparison between phases, we list the tensors corresponding to all the symmetry-inequivalent atoms of the FE phase. Atoms are labeled as in Table I.

Atom	$Cmcm$ (PE)	$Cmc2_1$ (FE)
La(1)	$\begin{pmatrix} 4.63 & 0 & 0 \\ 0 & 4.17 & 0 \\ 0 & 0 & 4.72 \end{pmatrix}$	$\begin{pmatrix} 4.64 & 0 & 0 \\ 0 & 4.09 & -0.21 \\ 0 & -0.69 & 4.71 \end{pmatrix}$
La(2)	$\begin{pmatrix} 4.37 & 0 & 0 \\ 0 & 3.76 & 0 \\ 0 & 0 & 4.28 \end{pmatrix}$	$\begin{pmatrix} 4.63 & 0 & 0 \\ 0 & 4.13 & 0.41 \\ 0 & 0.24 & 4.24 \end{pmatrix}$
Ti(1)	$\begin{pmatrix} 6.91 & 0 & 0 \\ 0 & 6.70 & 0 \\ 0 & 0 & 5.72 \end{pmatrix}$	$\begin{pmatrix} 6.16 & 0 & 0 \\ 0 & 5.60 & -0.36 \\ 0 & 0.24 & 5.31 \end{pmatrix}$
Ti(2)	$\begin{pmatrix} 6.33 & 0 & 0 \\ 0 & 5.32 & 0 \\ 0 & 0 & 7.45 \end{pmatrix}$	$\begin{pmatrix} 6.11 & 0 & 0 \\ 0 & 5.29 & 0.09 \\ 0 & -0.15 & 6.32 \end{pmatrix}$
O(1)	$\begin{pmatrix} -2.52 & 0 & 0 \\ 0 & -3.20 & 0.73 \\ 0 & 0.86 & -3.26 \end{pmatrix}$	$\begin{pmatrix} -2.52 & 0 & 0 \\ 0 & -3.14 & 0.53 \\ 0 & 0.38 & -2.92 \end{pmatrix}$
O(2)	$\begin{pmatrix} -2.52 & 0 & 0 \\ 0 & -3.20 & -0.73 \\ 0 & -0.86 & -3.26 \end{pmatrix}$	$\begin{pmatrix} -2.15 & 0 & 0 \\ 0 & -2.35 & -0.89 \\ 0 & -0.90 & -3.44 \end{pmatrix}$
O(3)	$\begin{pmatrix} -2.08 & 0 & 0 \\ 0 & -3.27 & -1.72 \\ 0 & -1.56 & -3.98 \end{pmatrix}$	$\begin{pmatrix} -1.76 & 0 & 0 \\ 0 & -3.33 & -1.36 \\ 0 & -1.38 & -2.95 \end{pmatrix}$
O(4)	$\begin{pmatrix} -2.08 & 0 & 0 \\ 0 & -3.27 & 1.72 \\ 0 & 1.56 & -3.98 \end{pmatrix}$	$\begin{pmatrix} -2.49 & 0 & 0 \\ 0 & -3.19 & 1.28 \\ 0 & 1.19 & -3.64 \end{pmatrix}$
O(5)	$\begin{pmatrix} -2.49 & 0 & 0 \\ 0 & -3.15 & 1.19 \\ 0 & 0.98 & -3.64 \end{pmatrix}$	$\begin{pmatrix} -2.63 & 0 & 0 \\ 0 & -3.11 & 1.04 \\ 0 & 1.00 & -3.36 \end{pmatrix}$
O(6)	$\begin{pmatrix} -5.50 & 0 & 0 \\ 0 & -2.15 & 0 \\ 0 & 0 & -1.66 \end{pmatrix}$	$\begin{pmatrix} -5.04 & 0 & 0 \\ 0 & -2.08 & 0.24 \\ 0 & 0.14 & -1.75 \end{pmatrix}$
O(7)	$\begin{pmatrix} -5.10 & 0 & 0 \\ 0 & -1.73 & 0 \\ 0 & 0 & -2.41 \end{pmatrix}$	$\begin{pmatrix} -4.99 & 0 & 0 \\ 0 & -1.91 & -0.03 \\ 0 & -0.02 & -2.20 \end{pmatrix}$

Then, we used the effective-charge tensors of the $Cmcm$ phase (given in Table IV) to compute the polarization change associated with the condensation of the $\boldsymbol{\xi}_1$ and $\boldsymbol{\xi}_2$ soft modes that dominate the $Cmcm$-to-$Cmc2_1$ transformation. The polar character of the modes is quantified in terms of the *mode effective charges*:

$$\bar{Z}_{s,\alpha} = \sum_{i\beta} Z^*_{i,\alpha\beta} \xi_{s,i\beta} \,. \tag{7}$$

We obtained $\bar{Z}_{1,z} = 1.8e$ and $\bar{Z}_{2,z} = 12.0e$, where e is the elemental charge. These results confirm that the $\boldsymbol{\xi}_1$ is weakly polar, in accordance with its AFD-like nature. In contrast, the second soft mode $\boldsymbol{\xi}_2$ is found to have a considerably polar character. It can then be trivially shown that the two soft modes have a very similar contribution to the total spontaneous polarization of the $Cmc2_1$ phase of LTO, in spite of the fact that $\boldsymbol{\xi}_1$ embodies 81% of the PE-to-FE distortion. Hence, the two-mode character of the FE distortion is critical to explain the relatively large $\boldsymbol{P}^S$ of the $Cmc2_1$ phase.

Unfortunately, we were unable to find experimental results for the FE and response properties of the $Cmc2_1$ phase of LTO. Table III shows some results for the $P2_1$ phase of the compound that is stable at room temperature. Interestingly, the dielectric and piezoelectric responses measured for this phase seem compatible (at least in magnitude) with our values for $Cmc2_1$. As regards the spontaneous polarization, the value for the $P2_1$ phase is smaller than ours by a factor of 6; this experimental result agrees well with the first-principles calculation of Ref. 16, which employed a DFT scheme similar to ours.[49] Hence, we can tentatively conclude that the $Cmc2_1$-to-$P2_1$ transformation, which is experimentally determined to occur at 1053 K,[34] involves a reduction of LTO's spontaneous polarization. While such a reduction in the magnitude of $\boldsymbol{P}^{\mathrm{S}}$ as the temperature decreases is not typical in FE perovskites, in principle there is no reason to question this possibility.

Finally, let us discuss an intriguing possibility suggested by the very different magnitudes of the computed mode charges $\bar{Z}_{1,z}$ and $\bar{Z}_{2,z}$. Since $\bar{\boldsymbol{Z}}_s$ quantifies the coupling between a polar mode and an applied electric field, we can expect $\boldsymbol{\xi}_2$ to be much more reactive to an external bias than $\boldsymbol{\xi}_1$. One can thus imagine the following possibility: to apply an electric field to LTO in its $Cmc2_1$ phase and switch *only the part of the spontaneous polarization associated with* $\boldsymbol{\xi}_2$. More precisely, if $(u_1^{\mathrm{I}},u_2^{\mathrm{I}})$ represents the FE phase discussed so far, an electric field might allow us to take the material into a qualitatively different polarization state $(u_1^{\mathrm{II}},u_2^{\mathrm{II}}) \approx (u_1^{\mathrm{I}}, -u_2^{\mathrm{I}})$. LTO would thus be a four-state FE, as the $(-u_1^{\mathrm{I}}, -u_2^{\mathrm{I}})$ and $(-u_1^{\mathrm{II}}, -u_2^{\mathrm{II}})$ variants would be accessible as well. A necessary condition for such a partial switching to occur is that the $(u_1^{\mathrm{II}},u_2^{\mathrm{II}})$ state be a minimum of the energy. More precisely, we need the coupling between $\boldsymbol{\xi}_1$ and $\boldsymbol{\xi}_2$ to be dominated by the $\gamma'' u_1^2 u_2^2$ term of Eq. (2): Note that, for $|\gamma''|$ much greater than $|\gamma'|$ and $|\gamma'''|$, the four states $(\pm u_1^{\mathrm{I}}, \pm u_2^{\mathrm{I}})$ would have essentially the same energy; in contrast, if γ' or γ''' dominates, the "$\boldsymbol{\xi}_2$-switched" state would have a much higher energy and might not be a minimum of $E(u_1,u_2)$. To confirm or disprove such a partial switching, we considered the equilibrium structure of the $Cmc2_1$ phase (i.e., the one reported in Table I) and generated configurations in which the $\boldsymbol{\xi}_2$ distortion was inverted and given various magnitudes; we relaxed such transformed structures and invariably obtained the original $Cmc2_1$ phase as the final result. Hence, while we did not explore the $E(u_1,u_2)$ energy landscape in detail, our results clearly indicate there is no stable $\boldsymbol{\xi}_2$-switched state. Equivalently, this implies that the γ' and γ''' terms of Eq. (2) dominate over γ'' (which supports the assumption made in Sec. III C).

E. $BaTiO_3$-like ferroelectric modes in $La_2Ti_2O_7$

Thus far we have discussed the main features of LTO's high-temperature FE transition, showing that this compound is very different from the FE oxides with the ideal perovskite structure. In particular, our results seem to suggest that LTO and BTO have little in common, in spite of the fact that they share the same building blocks: TiO_6 octahedra with Ti^{4+} in the $3d^0$ electronic configuration. In the following we show that such a conclusion would be a deceptive one.

TABLE V. Computed effective-charge tensors (given in units of elementary charge) for the $Pm\bar{3}m$ (PE) and $P4mm$ (FE) phases of BTO. The tensors are given in the conventional Cartesian axes for a rectangular lattice. They correspond to the following atoms (PE phase positions given in relative units): Ba located at (0,0,0), Ti at (1/2,1/2,1/2), O(1) at (1/2,1/2,0), and O(2) at (0,1/2,1/2). O(1) and O(2) are symmetry equivalent in the PE phase, but not in the z-polarized FE phase.

Atom	$Pm\bar{3}m$ (PE)	$P4mm$ (FE)
Ba	$\begin{pmatrix} 2.72 & 0 & 0 \\ 0 & 2.72 & 0 \\ 0 & 0 & 2.72 \end{pmatrix}$	$\begin{pmatrix} 2.71 & 0 & 0 \\ 0 & 2.71 & 0 \\ 0 & 0 & 2.81 \end{pmatrix}$
Ti	$\begin{pmatrix} 7.31 & 0 & 0 \\ 0 & 7.31 & 0 \\ 0 & 0 & 7.31 \end{pmatrix}$	$\begin{pmatrix} 7.05 & 0 & 0 \\ 0 & 7.05 & 0 \\ 0 & 0 & 5.83 \end{pmatrix}$
O(1)	$\begin{pmatrix} -2.13 & 0 & 0 \\ 0 & -2.13 & 0 \\ 0 & 0 & -5.77 \end{pmatrix}$	$\begin{pmatrix} -1.98 & 0 & 0 \\ 0 & -1.98 & 0 \\ 0 & 0 & -4.79 \end{pmatrix}$
O(2)	$\begin{pmatrix} -5.77 & 0 & 0 \\ 0 & -2.13 & 0 \\ 0 & 0 & -2.13 \end{pmatrix}$	$\begin{pmatrix} -5.62 & 0 & 0 \\ 0 & -2.14 & 0 \\ 0 & 0 & -1.96 \end{pmatrix}$

Ferroelectricity in the usual FE perovskite oxides relies on strong dipole-dipole interactions whose fingerprint is the anomalously large magnitude of the Born effective charges of some atomic species.[50] A prototypical example of this behavior is BTO, for which we computed the effective-charge tensors shown in Table V. Most notably, in the PE phase the Ti^{4+} cations display Z^* values above $7e$, almost doubling their nominal ionization charge. Analogously, the displacement of the O atoms toward the Ti has a dynamical charge of $-5.77e$ associated with it, almost tripling the nominal value of $-2e$. It is well known that this effect is related to a partial covalent character of the Ti–O bond, and an increased hybridization of the O-$2p$ and Ti-$3d$ orbitals as the Ti and O atoms approach.[17] Thus, given this chemical origin, the effective charges become less anomalous once the FE distortion freezes in: According to the results in Table V, Ti's charge of $7.31e$ gets reduced to $5.83e$, while O's charge of $-5.77e$ falls to $-4.79e$.

As is apparent from Table IV, some Ti and O atoms in LTO also present anomalously large effective charges that reach values similar to those obtained for BTO. In the case of the Ti atoms, the computed $\boldsymbol{Z}^*$ tensors are rather isotropic, with the maximum Z^* values [i.e., $6.91e$ for Ti(1) and $7.45e$ for Ti(2)] corresponding to displacements along the in-layer directions x and z. In the case of the O atoms, O(6) and O(7) clearly present the largest values, which exceed $-5e$ as in BTO. Such giant dynamical charges correspond to displacements along the x direction, for which LTO presents infinite chains of TiO_6 octahedra (see Figs. 1 and 2) such as those in the ideal perovskite structure. Hence, as regards their *polarizability* properties, the results for the Ti and O atoms in LTO are strongly reminiscent of the behavior that is well known for BTO.

Do such anomalous effective charges lead to FE instabilities in LTO? In accordance with the above discussion, the answer to this question is a negative one: The $Cmcm$ phase presents only two Γ-point instabilities (i.e., the already discussed $\boldsymbol{\xi}_1$ and $\boldsymbol{\xi}_2$) and the $Cmc2_1$ is stable against Γ-point perturbations. Hence, LTO is in this sense similar to the magnetic perovskite

$CaMnO_3$,[9] and provides a new example of a material in which the presence of anomalously large Born effective charges does *not* lead to a BTO-like FE instability.

Nevertheless, by inspecting the $\boldsymbol{K}$ eigenmodes of the $Cmcm$ phase, it is easy to find several low-energy FE modes that are BTO-like, i.e., they involve the displacement of the Ti atoms away from the center of nearly undistorted O_6 octahedra.[51,52] For example, we found a marginally stable and strongly polar mode for which we computed $\kappa_s = 0.26$ eV/Å^2 and $\bar{Z}_{s,x} = 21.7e$ (this distortion is x polarized and has B_{3u} symmetry); this mode gives an enormous contribution to the ϵ_{xx} dielectric response:[53] The obtained value exceeds 600. Interestingly, these BTO-like modes become stiffer in the $Cmc2_1$ phase; thus, they do not give raise to any anomalously large contribution to the dielectric response reported in Table III.

In conclusion, our analysis shows that LTO presents obvious traces of the FE instabilities of BTO. Such a *transferability* of instabilities was demonstrated by one of us in an hexagonal polymorph of BTO.[52] In that case, the FE phase transition was shown to be driven by soft modes that are an almost perfect match of the usual BTO-like FE instability. In LTO, such modes are very low in energy, but still stable; further, they clearly compete with the dominating AFD-like instability, and become stiffer once the $Cmcm$-to-$Cmc2_1$ transition occurs. Nevertheless, noting that BTO-like FE distortions tend to be very sensitive to cell strains, our results suggest the possibility that such instabilities might be induced in LTO by suitable strain engineering or chemical substitution (as has been predicted for the above-mentioned $CaMnO_3$)[9] or that they might occur spontaneously in similar layered perovskites.

F. Implications for work on magnetoelectrics

Finding materials that display large ME effects (i.e., a large magnetic reaction to an applied electric field) at room temperature is a major challenge that remains to be successfully tackled. The difficulties involved in the design of good magnetoelectrics have been discussed elsewhere.[54] At present, the strategies that seem most promising rely on finding systems that satisfy the following two conditions: (1) their atomic structure must react strongly to an applied electric field (i.e., we are looking for good dielectrics), and (2) the field-induced distortions must have a large effect on the magnetic interactions (as emphasized in Refs. 55 and 56).

While there are well-known strategies to comply with the first condition,[54] satisfying the second one is proving much more difficult. In fact, the existing quantitative studies indicate that the dielectric response of ME multiferroics like $BiFeO_3$ is dominated by modes that have small magnetostructural couplings associated with them.[57] It is thus interesting to consider the alternative approach adopted by Benedek and Fennie:[13] These authors noted that modes involving O_6 rotations are likely to be strongly coupled with the magnetism of perovskite oxides, as such AFD-like distortions usually control the nature and magnitude of the main magnetic interactions (e.g., the metal–oxygen–metal superexchange and Dzyaloshinskii–Moriya couplings). Hence, they looked for materials in which AFD-like distortions are related with (or lead to) ferroelectricity, as in such cases one could use an electric field to act on the O_6 rotations. Note that the sought connection between AFD-like distortions and ferroelectricity is an exotic one, since the O_6-rotational modes are strictly nonpolar in compounds with the ideal perovskite structure (see Sec. III B). Accordingly, ferroelectricity-related O_6-rotational modes have been found in nonideal perovskites, e.g., in the $PbTiO_3/SrTiO_3$ artificial superlattices[6] and the layered compound $Ca_3Mn_2O_7$.[13] In both cases, ferroelectricity has a *nonproper* character, and a combination of various modes must occur for a spontaneous polarization to appear.

Hence, our findings for LTO, and the analogous ones for the above- mentioned $BaMF_4$ fluorides,[21] are particularly important in the context of magnetoelectrics. In LTO's case, the FE soft mode is AFD-like already; hence it can freeze in and give rise to a sizable spontaneous polarization by itself, without the need of any accompanying distortion. Further, LTO's O_6 rotations couple directly (bilinearly) with an applied electric field, which might prove advantageous for the purpose of obtaining large ME effects. (In nonproper ferroelectrics, the coupling between an applied field and the AFD-like modes will typically be a higher-order effect.) Indeed, the *proper ferroelectricity driven by O_6 rotations* that occurs in LTO seems to be the ideal FE instability from the viewpoint of ME applications.

One would thus like to obtain LTO-like ferroelectricity in a magnetic oxide. The most obvious possibility is to consider the substitution of Ti by Mn in LTO, so as to form $La_2Mn_2O_7$, a crystal that we have not found described in the literature. In $La_2Mn_2O_7$ we would have manganese in the Mn^{4+} ionization state, most likely in the high-spin $t_{2g}^3 e_g^0$ electronic configuration; thus, we can expect this crystal to be insulating. Further, since the Ti–O chemistry does not seem to play any relevant role in LTO's FE instability, we can expect $La_2Mn_2O_7$ to present a FE transition analogous to LTO's. Hence, this material seems an excellent candidate to satisfy condition (2) mentioned above and thus to display large ME effects. Additionally, one would like the FE transition to occur near room temperature, so as to benefit from the enhancement of the functional responses near T_C [in the spirit of condition (1) mentioned above]. In this sense, it may be useful to note that materials like $Sr_2Ta_2O_7$[58] or $Sr_2Nb_2O_7$[59] present FE transitions that seem similar to LTO's but occur at lower T_C's: 166 and 1615 K, respectively. This suggests that exploring alternative compositions is a promising route to tune the temperature of the O_6-rotational FE transition.

IV. SUMMARY AND CONCLUSIONS

We used first-principles methods to study the origin of ferroelectricity in the layered perovskite $La_2Ti_2O_7$ (LTO), one of the materials with the highest Curie temperature known ($T_C = 1770$ K). To do so, we carried out for LTO a research program that has been repeatedly and successfully applied to the investigation of displacive phase transitions in ferroelectric (FE) oxides with the perovskite structure. Our results allowed us to characterize LTO's high-temperature FE transition, which was found to present a number of noteworthy features.

We found that ferroelectricity in LTO is very different from what occurs in the well-known FE oxides with the ideal perovskite structure, such as $BaTiO_3$ (BTO) or $PbZr_{1-x}Ti_xO_3$ (PZT). Indeed, the dominant FE instability of this compound

has little in common with the textbook picture of positive charges moving against negative charges in an ionic insulator; instead, it involves concerted rotations of the oxygen octahedra that form the perovskite framework. Hence, LTO's high-temperature structural transition is reminiscent of the behavior of simple perovskite oxides, but not the FE ones: LTO's FE distortion is much like the O_6-rotational soft modes that drive the *antiferrodistortive* phase transitions of $SrTiO_3$, $LaAlO_3$, $LaMnO_3$, and many other *nonpolar* perovskite crystals.

Hence we found that the existence of ferroelectricity in LTO at record-high temperatures is the result of structural distortions such as those occurring in many perovskite oxides that are *not* ferroelectric. As discussed here, the solution to this puzzle has to do with LTO's layered structure: Because the lattice of oxygen octahedra is truncated in this compound, the O_6 rotations acquire a polar character and give rise to a macroscopic polarization. We can thus describe LTO as a *topological ferroelectric*, since it owes its spontaneous polarization to the layered topology of its structure. Note that such a peculiar topology does not seem essential for LTO's high-temperature transition to occur, but it is critical for it to have a FE character. Interestingly, multiferroic barium fluorides $BaMF_4$ (where M = Mn, Fe, Co, or Ni) present the same sort of proper ferroelectricity;[21] indeed, such compounds belong to the same family of layered perovskites – with layers containing two, as opposed to four, perovskite-like planes – which further highlights the possibility of inducing FE behavior through the control of the lattice topology.

We quantified the energetics of LTO's FE transformation, the results being consistent with the very high temperature at which it happens. Most remarkably, we found that the structural distortion connecting the PE ($Cmcm$) and FE ($Cmc2_1$) phases presents large contributions from two modes, namely, the above-mentioned strong instability consisting of O_6 rotations and an isosymmetric weakly unstable mode that involves deformations of the oxygen octahedra. Further, we found that the large energy change associated with the $Cmcm$-to-$Cmc2_1$ transition depends crucially on the simultaneous occurrence of both modes. We were able to describe such effects in terms of a very strong and *cooperative* anharmonic coupling, and briefly discussed the possibility of constructing a phenomenological theory of such a *two-mode transition*. Interestingly, LTO's behavior is in strong contrast to what is most common among perovskite oxides, where structural instabilities tend to compete and suppress each other. Further, the investigated transition seems to align with other complex transformations recently discussed for various layered-perovskite oxides, such as those occurring in the Aurivillius compound $SrBi_2Ta_2O_9$[47] and Ruddlesden–Popper crystal $Ca_3Mn_2O_7$.[13] Hence, our results support the notion that such defected structures have a tendency to present *multimode* phase transitions.

We calculated the polarization and response properties of LTO's FE phase, obtaining results that are consistent with related experimental information. Interestingly, the computed electric properties revealed clear similarities between LTO and prototype FE BTO. For example, we obtained anomalously large Born effective charges for some Ti and O atoms in LTO, a feature that is known to be the fingerprint of the FE instabilities in compounds like BTO and PZT. Further, our results showed that LTO presents nearly unstable modes that are strongly polar and involve atomic distortions that essentially match BTO's FE instabilities. Such traces of BTO-like behavior in LTO suggest the intriguing possibility that *conventional* ferroelectricity might be induced in this compound upon suitable modifications (e.g., strain engineering or chemical substitutions) or that such a behavior might occur spontaneously in similar materials.

Finally, let us emphasize the implications that our findings have for the design of new ME multiferroics. In the context of ME perovskite oxides, it would be ideal to have proper ferroelectricity driven by O_6-rotational modes, so that an electric field can be used to tune the structural distortions (e.g., metal–oxygen–metal angles) that control the main magnetic interactions (i.e., superexchange and Dzyaloshinskii–Moriya). That is exactly the kind of ferroelectricity that we have found in LTO. Here we have briefly discussed how to obtain such an effect in a magnetic perovskite, proposing $La_2Mn_2O_7$ as the most promising candidate material.

In conclusion, our theoretical study of LTO has revealed a wealth of interesting effects, some of which may have important implications for current work on multifunctional oxides. We thus hope this study will stimulate further investigations of these layered perovskites and the novel functionalities that they may offer.

ACKNOWLEDGMENTS

This work was supported by the EC-FP7 project OxIDes (Grant No. CP-FP 228989-2), MICINN-Spain (Grants Nos. MAT2010-18113, MAT2010-10093-E, and CSD2007-00041), and CSIC's JAE-preprogram (J.L.P.). We used the supercomputing facilities provided by CESGA, the tools provided by the Bilbao Crystallographic Server,[60] and the VESTA software[61] for the preparation of some figures. We gratefully acknowledge discussions with E. Canadell, C. Ederer, J. M. Pérez-Mato, M. Stengel, and J. C. Wojdeł.

[1] M. E. Lines and A. M. Glass, *Principles and Applications of Ferroelectrics and Related Materials* (Oxford University Press, New York, 1977, 2001).

[2] G. A. Samara, Solid State Phys. **56**, 240 (2001).

[3] K. M. Rabe, C. H. Ahn, and J.-M. Triscone, eds., *Physics of Ferroelectrics, A Modern Perspective* (Springer-Verlag, Berlin, Heidelberg, 2007).

[4] K. M. Rabe and P. Ghosez, Top. Appl. Phys. **105**, 117 (2007).

[5] J. Junquera and P. Ghosez, J. Comp. Theor. Nanosci. **5**, 2071 (2008).

[6] E. Bousquet, M. Dawber, N. Stucki, C. Lichtensteiger, P. Hermet, S. Gariglio, J.-M. Triscone, and P. Ghosez, Nature London **452**, 732 (2008).

[7] M. Fiebig, J. Phys. D: Appl. Phys. **38**, R123 (2005).

[8] A. Filippetti and N. A. Hill, Phys. Rev. B **65**, 195120 (2002).

[9] S. Bhattacharjee, E. Bousquet, and P. Ghosez, Phys. Rev. Lett. **102**, 117602 (2009).
[10] G. Catalan and J. F. Scott, Adv. Mater. **21**, 2463 (2009).
[11] B. B. Van Aken, T. T. M. Palstra, A. Filippetti, and N. A. Spaldin, Nat. Mater. **3**, 164 (2004).
[12] C. J. Fennie and K. M. Rabe, Phys. Rev. B **72**, 100103 (2005).
[13] N. A. Benedek and C. J. Fennie, Phys. Rev. Lett. **106**, 107204 (2011).
[14] S. Nanamatsu, M. Kimura, K. Doi, S. Matsushita, and N. Yamada, Ferroelectrics **8**, 511 (1974).
[15] H. Yan, H. Ning, Y. Kan, P. Wang, and M. J. Reece, J. Am. Ceram. Soc. **92**, 2270 (2009).
[16] E. Bruyer and A. Sayede, J. Appl. Phys. **108**, 053705 (2010).
[17] M. Posternak, R. Resta, and A. Baldereschi, Phys. Rev. B **50**, 8911 (1994).
[18] P. Ghosez, E. Cockayne, U. V. Waghmare, and K. M. Rabe, Phys. Rev. B **60**, 836 (1999).
[19] F. Lichtenberg, A. Hernberger, K. Wiedenmann, and J. Mannhart, Prog. Solid State Chem. **29**, 1 (2001).
[20] C. N. R. Rao and B. Raveau, *Transition Metal Oxides*, 2nd ed. (Wiley, New York, 1998).
[21] C. Ederer and N. A. Spaldin, Phys. Rev. B **74**, 024102 (2006).
[22] R. D. King-Smith and D. Vanderbilt, Phys. Rev. B **49**, 5828 (1994).
[23] In several publications it is assumed that the high-temperature phase of LTO presents the $Cmcm$ space group, and the literature is cited for experimental proof of this fact. However, we have carefully checked the literature and were unable to find any results concerning the crystal structure of LTO's PE phase.
[24] S. C. Abrahams and E. T. Keve, Ferroelectrics **2**, 129 (1971).
[25] E. Kroumova, M. I. Aroyo, and J. M. Pérez-Mato, Acta Crystallogr. Sec. B **58**, 921 (2002).
[26] E. Kroumova, M. I. Aroyo, J. M. Pérez-Mato, S. Ivantchev, J. M. Igartua, and H. Wondratschek, J. Appl. Crystallogr. **34**, 783 (2001); We also used the tools available in the "Materials Studio" software package (Accelrys, Inc.).
[27] S. C. Abrahams, S. K. Kurtz, and P. B. Jamieson, Phys. Rev. B **172**, 551 (1968).
[28] S. Nanamatsu, M. Kimura, K. Doi, and M. Takahashi, J. Phys. Soc. Jpn. **30**, 300 (1971).
[29] J. K. Brandon and H. D. Megaw, Philos. Mag. **21**, 189 (1970).
[30] H. W. Schmalle, T. Williams, A. Reller, A. Linden, and J. G. Bednorz, Acta Crystallogr. Sec. B **49**, 235 (1993).
[31] G. Kresse and J. Furthmuller, Phys. Rev. B **54**, 11169 (1996); G. Kresse and D. Joubert, *ibid.* **59**, 1758 (1999).
[32] P. E. Blochl, Phys. Rev. B **50**, 17953 (1994); G. Kresse and D. Joubert, *ibid.* **59**, 1758 (1999).
[33] X. Wu, D. Vanderbilt, and D. R. Hamann, Phys. Rev. B **72**, 035105 (2005).
[34] N. Ishizawa, F. Marumo, S. Iwai, M. Kimura, and T. Kawamura, Acta Crystallogr. Sec. B **38**, 368 (1982).
[35] A. M. Glazer, Acta Crystallogr. Sec. B **28**, 3384 (1972).
[36] P. M. Woodward, Acta Crystallogr. Sec. B **53**, 32 (1997).
[37] P. M. Woodward, Acta Crystallogr. Sec. B **53**, 44 (1997).
[38] C. Howard and H. T. Stokes, Acta Crystallogr. Sec. A **61**, 93 (2004).
[39] See, e.g., O. Diéguez, O. E. González-Vázquez, J. C. Wojdeł, and J. Íñiguez, Phys. Rev. B **83**, 094105 (2011), and references therein.
[40] In the usual perovskite oxides, the coupling between the FE modes and strain tends to be stronger than the AFD-strain coupling. For example, Fig. 1 of Ref. 9 illustrates these effects as computed for $CaMnO_3$; the FE-strain coupling is very significant, while the AFD-strain interaction is almost negligible. These couplings have been quantified in detail for $SrTiO_3$: King-Smith and Vanderbilt[22] computed FE-strain couplings of about 0.0036 hartree/bohr^5, while N. Sai and D. Vanderbilt [Phys. Rev. B **62**, 13942 (2000)] obtained AFD-strain couplings of about 0.0002 hartree/bohr^5.
[41] The fourth-order expression in Eq. (2) may not be a good description of the energy for arbitrary values of u_1 and u_2; e.g., distortions with $u_1 = u_2$ are unbounded from below for the fitted parameter values. An acceptable description of the full $E(u_1,u_2)$ energy landscape would probably require including higher-order terms.
[42] Usually, the lowest-order coupling term between two modes v and w with different symmetries is of the form u^2w^2; the modes compete if the coefficient for this term is positive and cooperate if it is negative. In the case of two isosymmetric modes, we also have terms of the form uw^3 and u^3w, which result in a cooperation between the modes irrespective of the sign of the associated coefficient. It is thus tempting to conclude that two isosymmetric modes always cooperate. One should not forget, though, that the magnitude of such coefficients will be small (and the *positive* coefficient of the u^2w^2 term will be large) if the two isosymmetric distortions are incompatible for whichever chemical or physical reason. Indeed, only physical and chemical mechanisms, and not symmetry, can lead to meaningful competition or cooperation between modes.
[43] W. Zhong and D. Vanderbilt, Phys. Rev. Lett. **74**, 2587 (1995).
[44] The soft character of the $\boldsymbol{\xi}_2$ mode is essential for it to have a strong impact on the energetics of the FE instability. To illustrate this point, let us imagine that $\boldsymbol{\xi}_2$ is a relatively hard mode with a typical value for the stiffness (e.g., $\kappa_2 = 10$ meV/Å^2) and the computed strong coupling with $\boldsymbol{\xi}_1$ (i.e., $\gamma' = -0.35$ eV/Å^4). In that case, the fully relaxed FE phase (i.e., the $\boldsymbol{\xi}_1 + \boldsymbol{\xi}_2$ minimum of the corresponding $\Delta \boldsymbol{X}$ curve) would lie about -0.46 meV/Å^3 below the PE structure. Hence, the effect of such a nonsoft $\boldsymbol{\xi}_2$ mode would be a small one, as the $\boldsymbol{\xi}_1$-only FE minimum lies at -0.44 meV/Å^3. Note also that, for the computed soft $\boldsymbol{\xi}_2$, the $\boldsymbol{\xi}_1 + \boldsymbol{\xi}_2$ FE minimum is about -0.94 meV/Å^3 below the PE phase.
[45] In the spirit of phenomenological Landau theory, we assume that a primary order parameter Q_1 can be identified and considered to be decoupled from all other modes, including isosymmetric ones, at the harmonic level. Accordingly, there is no Q_1Q_2 bilinear term in Eq. (3).
[46] The $Q_1^3Q_2$ term guarantees that both Q_1 and Q_2 will freeze in at T_C.
[47] J. M. Pérez-Mato, M. Aroyo, A. García, P. Blaha, K. Schwarz, J. Schweifer, and K. Parlinski, Phys. Rev. B **70**, 214111 (2004).
[48] R. D. King-Smith and D. Vanderbilt, Phys. Rev. B **47**, 1651 (1993).
[49] Comparing our results for the spontaneous polarization with those of Ref. 16 is not straightforward, for two reasons. First, the authors of Ref. 16 used a generalized-gradient approximation (GGA) to DFT. As compared with the LDA employed in this work, GGA is known to overestimate the structural distortion and spontaneous polarization in the usual FE perovskites – see, e.g., D. I. Bilc, R. Orlando, R. Shaltaf, G. M. Rignanese, J. Íñiguez, and P. Ghosez, Phys. Rev. B **77**, 165107 (2008), and references therein – and it is not clear whether something similar might occur in LTO. Second, the result reported in Ref. 16 was computed as the polarization difference between LTO's $P2_1$ phase and a hypothetical nonpolar structure with $P2_1/m$ symmetry. Hence, the polarization of the $P2_1$ phase was obtained using a reference different from ours.
[50] W. Zhong, R. D. King-Smith, and D. Vanderbilt, Phys. Rev. Lett. **72**, 3618 (1994).

[51]To quantify the resemblance between the TiO_6 distortions in BTO and LTO, we projected the corresponding atomic displacements of the $\boldsymbol{K}$ eigenmodes of LTO's $Cmcm$ phase into the distortion pattern derived from the FE soft mode of BTO's $Pm\bar{3}m$ phase. This kind of analysis is described in more detail in Ref. 52.

[52]J. Íñiguez, A. García, and J. M. Pérez-Mato, J. Phys. Condens. Matter **12**, L387 (2000).

[53]The lattice dielectric response can be split into mode contributions as $\epsilon_{\alpha\beta} = \Omega^{-1} \sum_s \bar{Z}_{s,\alpha} \bar{Z}_{s,\beta} \kappa_s^{-1}$, in units of ϵ_0 and where Ω is the cell, volume.

[54]J. C. Wojdeł and J. Íñiguez, Phys. Rev. Lett. **105**, 037208 (2010).

[55]C. J. Fennie, Phys. Rev. Lett. **100**, 167203 (2008).

[56]K. T. Delaney, M. Mostovoy, and N. A. Spaldin, Phys. Rev. Lett. **102**, 157203 (2009).

[57]J. C. Wojdeł and J. Íñiguez, Phys. Rev. Lett. **103**, 267205 (2009).

[58]N. Ishizawa, F. Marumo, T. Kawamura, and M. Kimura, Acta Crystallogr. Sec. B **32**, 2564 (1976).

[59]N. Ishizawa, F. Marumo, T. Kawamura, and M. Kimura, Acta Crystallogr. Sec. B **31**, 1912 (1975).

[60]M. I. Aroyo, J. M. Pérez-Mato, C. Capillas, E. Kroumove, S. Ivantchev, G. Madariaga, A. Kirov, and H. Wondratschek, Z. Kristallogr. **221**, 15 (2006); M. I. Aroyo, A. Kirov, C. Capillas, J. M. Perez-Mato, and H. Wondratschek, Acta Crystallogr. Sec. A **62**, 115 (2006).

[61]K. Momma and F. Izumi, J. Appl. Crystallogr. **41**, 653 (2008).